Journal of Chemotherapy

ISSN: (Print) (Online) Journal homepage: www.tandfonline.com/journals/yjoc20

Developing new drugs for adult T-cell leukemia/lymphoma by targeting hypoxia: insights from toxicity of MS-275 and its analogs

Sajad Goudarzi, Mohamad Vosough Ghanbari, Jalil Rohani, Razieh Ghodsi & Fatemeh B. Rassouli

To cite this article: Sajad Goudarzi, Mohamad Vosough Ghanbari, Jalil Rohani, Razieh Ghodsi & Fatemeh B. Rassouli (07 Oct 2024): Developing new drugs for adult T-cell leukemia/lymphoma by targeting hypoxia: insights from toxicity of MS-275 and its analogs, Journal of Chemotherapy, DOI: 10.1080/1120009X.2024.2411825

To link to this article: https://doi.org/10.1080/1120009X.2024.2411825

Published online: 07 Oct 2024.

JOURNAL OF CHEMOTHERAPY
https://doi.org/10.1080/1120009X.2024.2411825

Taylor & Francis
Taylor & Francis Group

RESEARCH ARTICLE

Developing new drugs for adult T-cell leukemia/lymphoma by targeting hypoxia: insights from toxicity of MS-275 and its analogs

Sajad Goudarzi[a], Mohamad Vosough Ghanbari[b], Jalil Rohani[b], Razieh Ghodsi[c,d] and Fatemeh B. Rassouli[a]

[a]Novel Diagnostics and Therapeutics Research Group, Institute of Biotechnology, Ferdowsi University of Mashhad, Mashhad, Iran; [b]Department of Medical Biotechnology and Nanotechnology, Faculty of Medicine, Mashhad University of Medical Sciences, Mashhad, Iran; [c]Biotechnology Research Center, Pharmaceutical Technology Institute, Mashhad University of Medical Sciences, Mashhad, Iran; [d]Department of Medicinal Chemistry, School of Pharmacy, Mashhad University of Medical Sciences, Mashhad, Iran

ABSTRACT

The low survival rate of adult T-cell leukemia/lymphoma (ATL) underscores the critical need for innovative therapeutic agents. While the pharmacokinetics of HDACis have been documented in several hematological neoplasms, there is a notable gap in research regarding their activity against ATL. Given that hypoxia can induce unpredictable effects on lymphoma cells, this study aimed to evaluate the toxic effects of MS-275 and novel analogs on ATL cells in hypoxic condition for the first time. Protein-protein interaction and gene set enrichment analyses were performed, the expression of HIF1A and downstream targets were assessed, and molecular docking was conducted on MS-275 and novel analogs with HIF-1α. For *in vitro* studies, at first benzamide analogs of MS-275 were synthesized and then, viability of MT-2 cells was evaluated in hypoxic condition. Enrichment analyses confirmed the involvement of hub genes in HIF-1 signaling pathway and volcano plot revealed over expression of HIF1A, GAL3ST1 and CD274. Molecular docking indicated favorable interaction between MS-275 and analogs with HIF-1α PAS-B domain. Results of alamarBlue assay demonstrated that MS-275 and analogs significantly ($p < 0.001$) reduced viability of MT-2 cells in hypoxic condition. Findings of the present study hold promise for developing new drugs targeting hypoxia-induced changes in ATL.

ARTICLE HISTORY
Received 13 July 2024
Revised 5 September 2024
Accepted 27 September 2024

KEYWORDS
MS-275; histone deacetylase inhibitor; HIF-1α; adult T-cell leukemia/lymphoma; MT-2 cells

Introduction

Histone deacetylase inhibitors (HDACis) are a class of drugs that target the aberrant epigenetic characteristics of neoplastic cells. By regulating chromatin accessibility for transcription factors, HDACis fine-tune the transcriptional activity of genes involved in development, cellular homeostasis, and cancer progression [1]. Accordingly, HDACis have emerged as promising anticancer agents and their potential against tumor progression has been shown on several solid tumors and hematological malignancies [2]. Currently, four HDACis have received FDA approval: SAHA for cutaneous T-cell lymphoma, PXD101 for peripheral T-cell lymphoma, LBH589 for multiple myeloma, and FK-228 for peripheral T-cell lymphoma [3–6].

HDACis are classified into five structural categories, including benzamides, hydroximates, cyclic tetrapeptides, aliphatic acids, and electrophilic ketones. MS-275, also referred to as SNDX-275, is a benzamide-like, zinc-dependent HDACi. Its structure is composed of three key domains: a cap group or surface recognition unit, a zinc binding domain (ZBD) and a linker domain that connects the cap and ZBD. The cap and linker domains contribute to ligand-receptor interactions and affect the selectivity of HDACi, while binding of the ZBD to zinc in the HDAC active site plays a decisive role in the inhibitory activity of HDACi [7]. We have recently designed and synthesized novel MS-275 analogs possessing the cap pyridine ring, benzamid linker and o-phenylenediamine as ZBD [8,9].

As an orally bioavailable HDACi, MS-275 has potent anti-tumor activity, and exhibits great selectivity as it specifically targets class I and class IV HDACs [10,11]. While MS-275 has shown promise in the treatment of Hodgkin lymphoma, acute myeloid leukemia, and chronic myelomonocytic leukemia [12–15], further research is required to fully understand the efficacy

CONTACT Fatemeh B. Rassouli behnam3260@um.ac.ir Novel Diagnostics and Therapeutics Research Group, Institute of Biotechnology, Ferdowsi University of Mashhad, Mashhad, Iran

and potential clinical applications of MS-275 in other hematological malignancies.

Adult T-cell leukemia/lymphoma (ATL) is an invasive neoplasm originating from post-thymic regulatory T-cells, which is caused by oncoretroviral human T-cell leukemia virus type 1 (HTLV-1). ATL exhibits diverse presentations, characterized by varying degrees of leukemic and/or lymphomatous involvement [16]. ATL is classified according to the Shimoyama classification into four subtypes: acute, lymphomatous, chronic and smoldering, which show the highest to lowest prevalence, respectively [17]. The prognosis of ATL varies across clinical subtypes, with the most aggressive forms, acute and lymphomatous, yield survival times of less than 1 year. However, the slower-growing subtypes, smoldering and chronic, extend survival to approximately 2 years [18].

Tissue hypoxia arises from an imbalance between local oxygen consumption and supply, stemming from factors such as increased cellular activity or reduced perfusion. At the cellular level, hypoxic stress triggers adaptation mechanisms, with hypoxia-inducible transcription factors (HIFs) being pivotal. HIF-1α plays a crucial role in tumor development by regulating the expression of genes involved in cell proliferation and apoptosis, angiogenesis, glucose metabolism, immune response, and therapeutic resistance. Beyond solid tumors, growing evidence suggests that HIF-1α is also intimately linked with the development and progression of hematological malignancies, such as leukemia, lymphoma and multiple myeloma [19]. T lymphocytes are commonly confronted with hypoxia, since thymocytes are present in relatively hypoxic regions during T-cell development [20]. On the other hand, hypoxia influences the appearance and clinical behavior of lymphoma, as oxygen deficiency transforms the hypoxic region into localized necrosis, which is common in invasive lymphomas [21]. Moreover, hypoxia induces the expression of programmed death ligand-1 (PD-L1/CD274) and galactose-3-O-sulfotransferase 1 (GAL3ST1), leading to immunosuppression by interfering with regulatory T cells [22,23].

The low survival rate of ATL underscores the critical need for innovative therapeutic agents. While the pharmacokinetics of HDACis have been documented in various hematological malignancies, there is a notable gap in research regarding their activity against ATL. Given that hypoxia can induce unpredictable effects on the viability of lymphoma cells, this study aimed to evaluate the effects of MS-275 and novel analogs on the viability of ATL cells in hypoxic condition by computational analysis and *in vitro* studies.

Materials and methods

Protein-protein interaction and gene set enrichment analysis

For construction of the protein-protein interaction networks, at first target genes of the HIF-1α transcription factor were retrieved from Harmonizome 3.0 (https://maayanlab.cloud/Harmonizome/gene_set), which consolidates data from the CHEA Transcription Factor Targets dataset. Additionally, genes associated with ATL were obtained from GeneCards (https://www.genecards.org), a database that integrates comprehensive information on all annotated and predicted human genes. To identify overlapping gene targets between HIF-1α and ATL, we intersected the data using a Venn diagram tool (https://bioinformatics.psb.ugent.be/webtools/Venn/). The protein-protein interaction for the overlapping gene set was constructed by STRING (https://string-db.org/), which combines both physical and functional associations. The interactome was also visualized using Cytoscape software (version 3.10.1), and the CytoHubba v0.1 plugin was employed to pinpoint key genes within the network.

To assess the biological relevance of the overlapped targets, gene set enrichment analysis was performed using ShinyGO (http://bioinformatics.sdstate.edu/go/), a web-based tool that calculates the false discovery rate (FDR) for a statistically robust evaluation. This analysis facilitated the identification of central genes and their functional roles within KEGG pathways and biological processes.

Data collection from gene expression omnibus

To identify differentially expressed genes between acute ATL and normal samples, microarray data were retrieved from Gene Expression Omnibus (GEO), which is a repository containing high-throughput functional genomic data (http://www.ncbi.nlm.nih.gov/geo). To find a gene expression dataset for ATL, we employed the following customized criteria: 'ATL' and 'Healthy control' as keywords, 'Homo sapiens' as the organism, and 'Expression profiling by array' as the study type. The gene expression data utilized in this study, accession number GSE55851 (platform GPL10332), were originally published by Nakano et al. (2014) [24]. The data analysis was performed using R (version 4.4.0) with the 'GEOquery' and 'limma' packages. The p values were adjusted using the Benjamini & Hochberg method to control the false discovery rate. A volcano plot was generated using the 'ggplot2' package in R, with a significance threshold of $p < 0.05$ and a $\log_2$ fold change ($\log_2$FC) > 1.

Molecular docking

To predict the binding interactions between MS-275 and its analogs with the HIF-1α, molecular docking was performed. The 3D structure of MS-275 (CID: 4261) was retrieved from PubChem (https://pubchem.ncbi.nlm.nih.gov/). For analogs, at first SMILE codes were generated by Mathpix online platform (https://snip.mathpix.com/home), and then PDB format files were obtained from the National Cancer Institute's website (https://cactus.nci.nih.gov/translate/). Ligand preparation involved energy minimization steps to optimize the structures. Crystal structure of the HIF-1α protein (ID: 4h6j) was retrieved from Protein Data Bank (https://www.rcsb.org/). Molecular docking was conducted using CB-Dock2 (https://cadd.labshare.cn/cb-dock2/index.php), a web server built on the AutoDock Vina 1.2.0 algorithm. This platform utilizes the robust and efficient AutoDock Vina method, renowned for its accuracy in predicting protein-ligand interactions. The tool facilitates the prediction of binding affinities by evaluating the free energy of binding, which quantitatively assesses the ligand's affinity for the protein. The docking results were thoroughly analyzed and visualized in both 2D and 3D formats using the Discovery Studio program, enabling the identification of critical residues and the precise spatial orientation of the ligand within the binding site of the protein.

Synthesis of analogs

Two analogs of MS-275 were synthesized as recently reported. For analog 1, N-(4-((2-aminophenyl)carbamoyl) benzyl)-6,7-dimethoxy-2-methylquinoline-4-carboxamide, 2-methylquinoline-4-carboxylic acid derivative coupled with 4-(aminomethyl) benzoic acid was produced. Synthesis of analog 2, N-(2-aminophenyl)-2-(4-fluorophenyl)quinoline-4-carboxamide, was carried out by a reaction between quinoline-4-carboxylic acid derivative and o-phenylenediamine [8, 9]. The chemical structures of both analogs were characterized using ^{1}H NMR,^{13}C NMR (Bruker FT-300 MHz instrument), infrared spectra (Perkin Elmer Model 1420 spectrometer) and mass spectra (A 3200 QTRAP LC/MS triple quadrupole mass spectrometer).

Cell treatment and viability assay

To investigate the effects of MS-275 and novel analogs, HTLV-1 transformed human T cells, MT-2 cell line, were used. The cells were derived from normal human cord leukocytes of a healthy donor co-cultured with leukemic cells from an ATL patient [25]. MT-2 cells were obtained from Pasteur Institute (Tehran, Iran) and cultured in Roswell Park Memorial Institute-1640 medium supplemented with 10% fetal bovine serum (Gibco), 0.1% L-glutamine (Gibco), and 1% penicillin/streptomycin (Sigma).

For treatment of cells, at first stock solutions of MS-275 (MW: 376.4 g/mol), analog 1 (MW: 468 g/mol), and analog 2 (MW: 357 g/mol) were prepared using DMSO as solvent. Subsequently, 12.5, 25 and 50 μM of each agent were prepared using complete medium right before use. Cells were seeded at a density of 50,000 cells per well in 96-well plates, treated

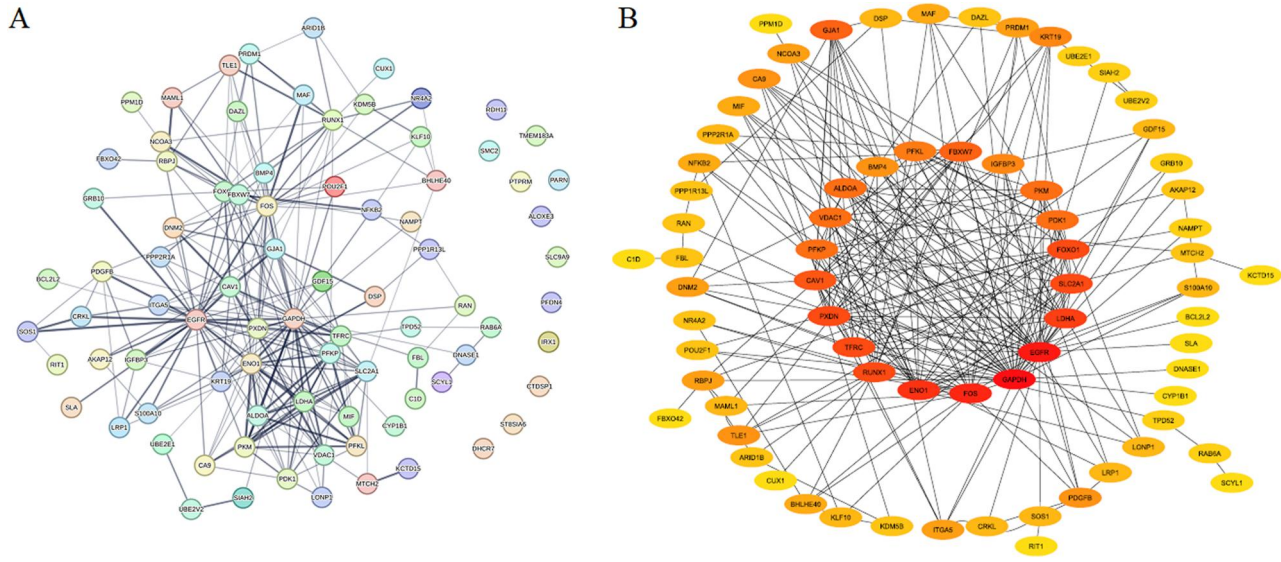

Figure 1. Protein-protein interaction network between overlapping targets of HIF-1α and ATL. STRING was used to map the interconnectedness of 84 proteins, identified through physical and functional interactions (a). Protein-protein interaction network with 72 nodes and 248 edges was constructed by and Cytoscape, in which the top 20 hub genes (nodes) were identified by the Cytohubba plugin (B).

with escalating concentrations of each agent, and incubated for 24 h at 37 °C in hypoxic condition (93% N_2, 5% CO_2, and 2% O_2, Binder). Untreated cells and cells treated with the same volume of DMSO (0.4% v/v) in all concentrations served as controls.

Viability of cells was evaluated using alamarBlue assay, where alamarBlue reagent (0.1 mg/ml, Sigma) was added to each well (10% v/v), and cells were incubated for 3 h at 37 °C. Absorbance (A) was measured at 600 nm (Epoch Biotek), and viability (%) was calculated using the following formula: 100-(AT-AU/AB-AU)*100, where T, U and B represent treated cells, untreated cells and blank control, respectively. Notably, cell viability assessments were performed in triplicate and repeated three times independently.

Statistical analysis

Data were statistically analyzed using one-way ANOVA in GraphPad Prism software. Results were presented as mean ± SD, and statistical significance was considered for p values less than 0.05, 0.01 and 0.0001.

Results

Web-based analysis revealed 304 target genes for HIF-1α and 3206 associated genes for ATL. Venn diagram analysis indicated 84 overlapping targets, upon which protein-protein interaction networks were constructed using STRING and Cytoscape. As illustrated in Figure 1, the network comprised 72 nodes and 248 edges. Based on their rankings in CytoHubba using the Degree method, the top 20 hub genes identified in the network were LDHA, RUNX1, FOS, VDAC1, GJA1, FOXO1, CAV1, PDK1, PFKP, SLC2A1, PXDN, ENO1, TFRC, IGFBP3, PFKL, EGFR, FBXW7, ALDOA, GAPDH and PKM.

The enrichment analysis of 20 hub genes revealed significant terms across multiple categories (Figure 2). In KEGG pathway analysis, hub genes were found to be significantly enriched in 'HIF-1 signaling pathway'

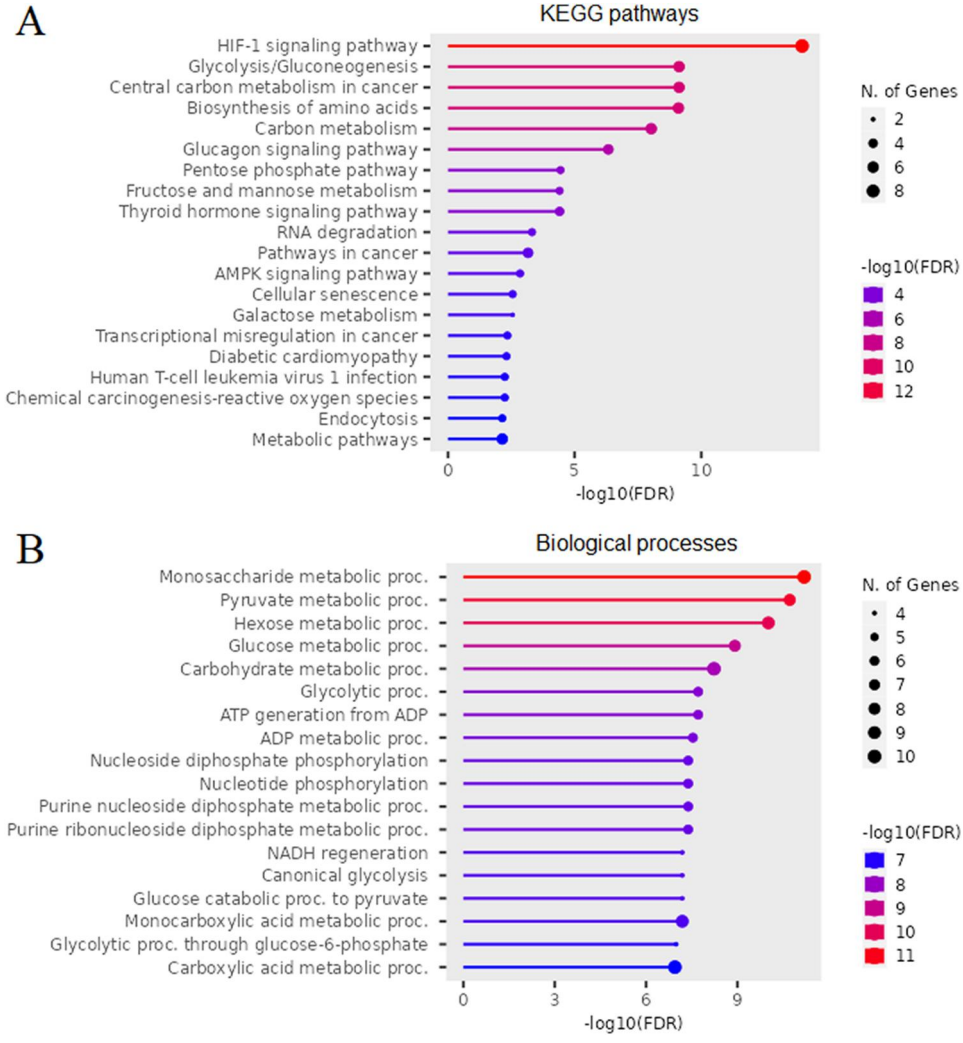

Figure 2. Enrichment and pathway analysis of overlapping 20 hub genes. The most significant KEGG pathways and terms of biological processes were visualized using ShinyGo online software.

(FDR: 1.04E-14, gene count: 9), 'Glycolysis/Gluconeogenesis' (FDR: 7.5E-10, Gene count: 6), and 'Central carbon metabolism in cancer' (FDR: 7.5E-10, Gene count: 6). In terms of biological processes, 'Monosaccharide metabolic processes' (FDR: 6.39E-12, gene count: 10) was identified as the most significant term. Additional pathways and terms were also obtained and presented in Table 1.

Due to the significance of hypoxia in lymphoma progression, the expression of HIF1A and two of its downstream targets, CD274 and GAL3ST1, was investigated in acute ATL using GSE5585. Employing R software on 22682 genes revealed significant over expression of HIF1A and GAL3ST1 in acute ATL samples in comparison with healthy volunteers. CD274 was also up regulated, although not significant (Figure 3).

To determine the interaction between MS-275 and analogs with HIF-1α PAS-B domain, molecular docking was performed. As shown in Figure 4 and summarized in Table 2, the interaction between MS-275 and HIF-1α consisted of two hydrogen bonds and several hydrophobic interactions with a binding affinity of −6.1 kJ/mol. The interaction of analog 1 and HIF-1α also exhibited stability, engaging in one hydrogen bond with a binding energy of −6.5 kJ/mol. Similarly, the interaction between analog 2 and HIF-1α consisted of one hydrogen bond with a binding affinity score of −6.2 kJ/mol. To note, CYS255 was among the interacted amino acids in all three dockings.

After identifying favorable interactions between MS-275 and analogs with HIF-1α, analog 1 and 2 were synthesized and viability of ATL cells was evaluated in hypoxic condition. As shown in Figure 5, all three agents exhibited toxic effects on MT-2 cells in a dose-dependent manner. The most significant ($p < 0.001$) effects were observed upon treatment of cells with 50 µM of MS-275, analog 1 and analog 2, and 73.4%, 64.2% and 68.2% viability was calculated, respectively.

Table 1. Gene set enrichment analysis of KEGG pathways and biological processes.

	Enrichment FDR	Fold Enrichment	Genes
KEGG pathways			
HIF-1 signaling pathway	1.04E-14	99.434	EGFR ENO1 ALDOA GAPDH PDK1 PFKL PFKP SLC2A1 TFRC
Glycolysis/Gluconeogenesis	7.50E-10	107.844	ENO1 ALDOA GAPDH PFKL PFKP PKM
Central carbon metabolism in cancer	7.50E-10	103.222	EGFR PDK1 PFKL PFKP PKM SLC2A1
Biosynthesis of amino acids	7.93E-10	97.642	ENO1 ALDOA GAPDH PFKL PFKP PKM
Carbon metabolism	9.45E-09	62.831	ENO1 ALDOA GAPDH PFKL PFKP PKM
Terms in biological processes			
Monosaccharide metabolic process	6.39E-12	269	PFKP PFKL PDK1 ENO1 FOXO1 PKM GAPDH IGFBP3 ALDOA SLC2A1
Pyruvate metabolic process	1.90E-11	114	PFKP PKM ENO1 GAPDH PFKL ALDOA PDK1 VDAC1
Hexose metabolic process	9.56E-11	250	PFKP PFKL PDK1 ENO1 FOXO1 PKM GAPDH IGFBP3 ALDOA
Glucose metabolic process	1.21E-09	207	PFKP PFKL PDK1 ENO1 FOXO1 PKM GAPDH IGFBP3
Carbohydrate metabolic process	5.85E-09	627	PFKP PKM ENO1 GAPDH PFKL ALDOA PDK1 FOXO1 IGFBP3 SLC2A1

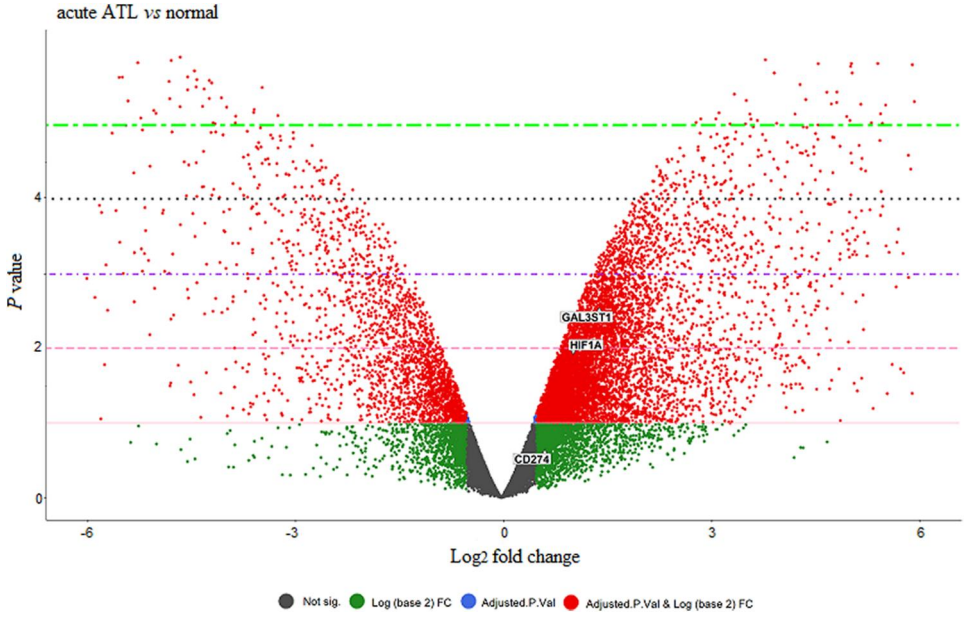

Figure 3. Volcano plot visualize the expression of HIF1A, GAL3ST1 and CD274 in GSE55851 dataset. The plot utilize both *p* value and log2 (fold-change) to identify differentially expressed genes in acute ATL.

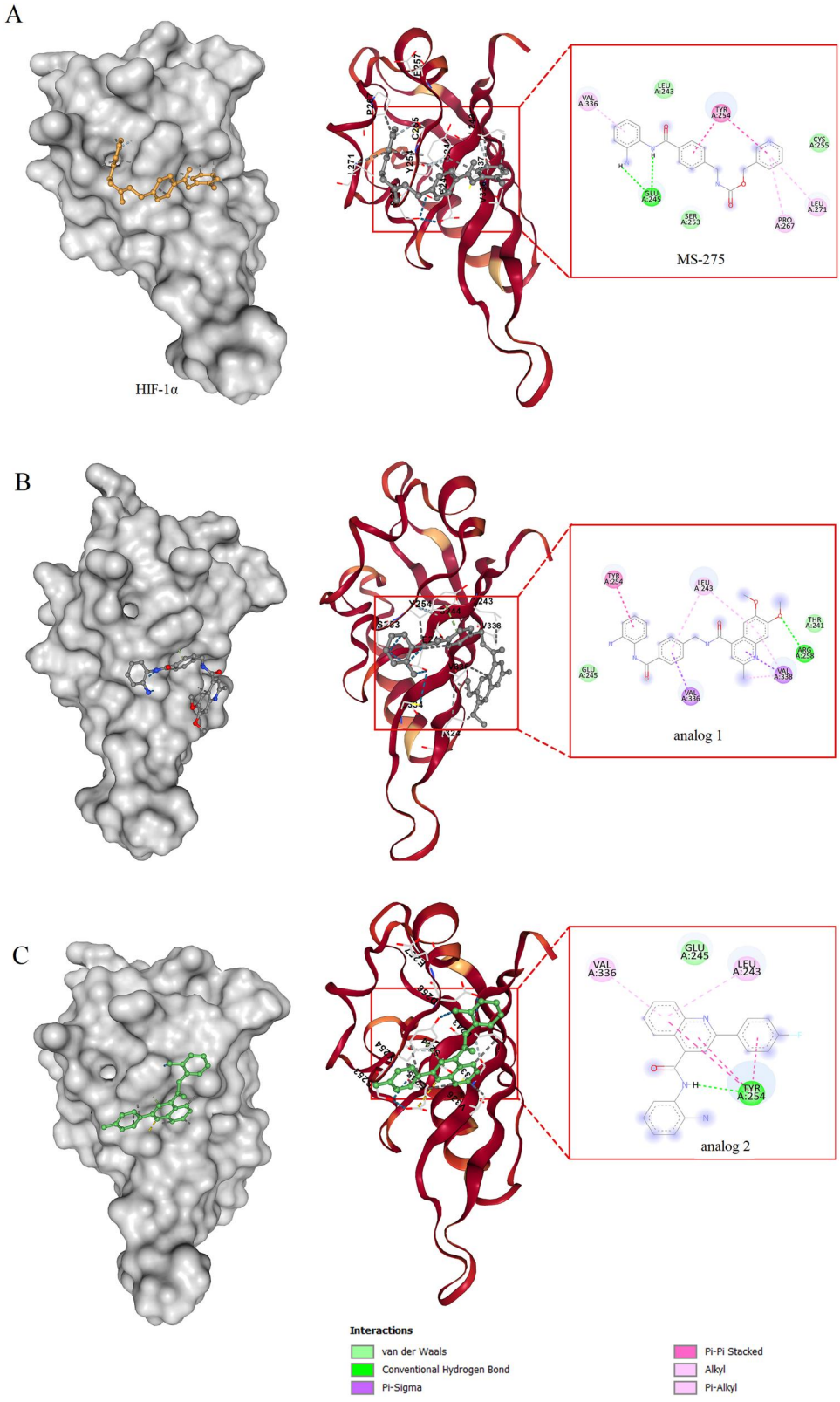

Figure 4. Molecular docking diagrams of MS-275 (a), analog 1 (B) and analog 2 (C) binding to HIF-1α PAS-B domain. 2D and 3D images were generated using Discovery Studio.

Discussion

Chemotherapy is the mainstay of treatment for ATL, however, patients who experience relapse or develop resistance to conventional chemotherapy have limited options and poor outcomes [26]. These limitations highlight the need for the development of novel therapeutic

Table 2. Docking scores and binding positions of MS-275, analog 1 and analog 2 with HIF-1α PASB domain.

Agent	Affinity (kJ/mol)	Hydrogen bond	Interacted amino acids
MS-275	−6.1	SER253, LU245	LEU243, SER244, GLU245, SER247, LYS251, PHE252, SER253, TYR254, CYS255, ASP256, GLU257, ARG258, PRO267, GLU268, LEU271, GLY272, ILE324, TYR325, ASN326, THR327, GLN333, CYS334, VAL336, CYS337
Analog 1	−6.5	RHR241	ASP238, LYS240, THR241, LEU243, SER244, GLU245, SER247, LYS251, PHE252, SER253, TYR254, CYS255, ASP256, GLU257, ARG258, PRO267, GLU268, LEU271, GLY272, ARG273, GLN320, ILE324, GLN333, VAL336, CYS337, VAL338, TYR340
Analog 2	−6.2	TYR254	THR241, LEU243, SER244, GLU245, SER253, TYR254, CYS255, ASP256, GLU257, ARG258, PRO267, LEU271, GLN299, GLN320, THR322, ILE324, CYS334, ILE335, VAL336, CYS337, VAL338

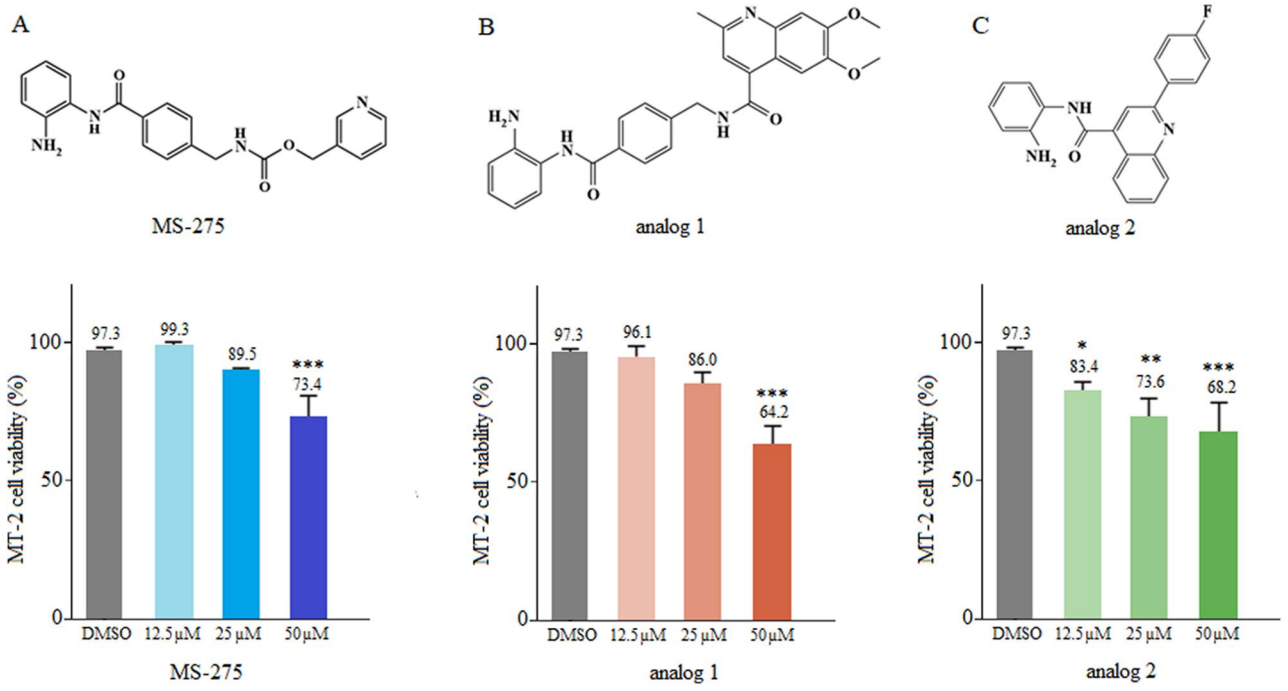

Figure 5. Viability assay of MT-2 cells following 24 h treatment with MS-275 (a), analog 1 (B) and analog 2 (C) in hypoxic condition. Results are presented as mean ± SD, and statistical significance is represented as $*p < 0.05$, $**p < 0.01$ and $***p < 0.0001$ in comparison with DMSO control.

strategies to improve treatment efficacy and minimize the detrimental impacts of routine approaches.

HDACs have been implicated as key pathogenic factors in various types of leukemia, such as chronic myeloid leukemia and chronic lymphocytic leukemia [27]. Although a number of HDACis have been developed for the treatment of hematological malignancies [3–6], the lack of a standard HDACi for ATL necessitates comprehensive studies. Preclinical studies have shown that AR-42, an orally bioavailable HDACi, reduced the proliferation of ATL cells by promoting apoptosis and enhanced the survival of ATL animal models [28]. Similarly, romidepsin, in single use and in combination with anti CD25 depsipeptide, prolonged survival in ATL murine models [29, 30]. In the first reported clinical trial, a combination of valproic acid (a first-generation HDACi) and AZT/IFN (as maintenance therapy) was tested in 13 ATL patients, which led to a decrease in clonal disease in only one patient [31]. Notably, ongoing trials are evaluating the efficacy of other HDACis, such as tucidinostat and belinostat, in ATL [32]. Given the significant role of hypoxia in ATL development and therapy resistance, we investigated effects of MS-275 and novel analogs on MT-2 cell viability in hypoxic condition for the first time.

HIF-1 is a basic helix-loop-helix heterodimer, consisting of an oxygen-sensitive HIF-1α subunit and a constitutively expressed HIF-β subunit. In normoxic condition, HIF-1α undergoes continuous degradation *via* ubiquitination and proteasomal pathways. In low-oxygen condition, however, HIF-1α becomes stable, hetrodimerizes with HIF-β and translocates to the nucleus, where it induces the expression of genes linked to chemotherapy resistance and immune evasion [22,23]. In the present study, intersection of targets for HIF-1α and ATL identified 84 overlapping genes. Enrichment analyses further confirmed that 20 of these genes act as hubs, participating in multiple

pathways and biological processes, including the HIF-1 signaling pathway and monosaccharide metabolism. In addition, volcano plot generated from acute ATL expression profile in the GEO dataset revealed over expression of HIF1A and its downstream genes GAL3ST1 and CD274.

The X-ray crystallography analysis of HIF-1α and HIF-β complex reveals that the heterodimeric interaction between these two subunits occurs through their PAS-B domain [33]. Molecular docking analysis predicted that MS-275 and novel analogs favorably interacted with HIF-1α PAS-B domain. Specifically, all interactions involved CYS255, which is essential for the interaction between two subunits [34]. Furthermore, *in vitro* analysis of cell viability indicated considerable toxicity of MS-27 and analogs on ATL cells in hypoxic condition. Our findings are in line with previous reports on MS-275 toxicity. For instance, it has been shown that MS-275 induced anti-proliferative and apoptosis-inducing effects on Hodgkin lymphoma cell lines *via* altering the expression of P21, BCL-2, and BCL-xL [13]. In addition, MS-275 up regulated the expression of c-Jun, JunB and death receptor TRAIL, and induced apoptosis in acute myeloid leukemia cells [35]. Other studies have also shown that combinatorial use of MS-275 with fludarabine or cladribine induced anti-proliferative and cytotoxic effects on chronic lymphocytic leukemia and multiple myeloma cells [14,15]. Similar to the current attempt, the bicyclic aromatic ring of MS-275 was used to design and synthesize class I HDACis, and *in vitro* assay identified an analog with superior anti-proliferative effects against human cutaneous T-cell lymphoma, leukemia, breast, cervical, colorectal, and gastric carcinomas [36]. Accordingly, quinoline-based benzamide analogs of MS-275 could be considered as promising candidates to develop novel drugs for hematological neoplasms.

The present study has certain limitations that warrant further investigation. As benzamide derivatives, MS-275 and its analogs exhibit limited aqueous solubility due to their relatively non-polar nature. This necessitated the use of DMSO to prepare the stock solutions in the current study, restricting the range of applied concentrations to 50 μM, despite the observed mild to moderate impact on viability. To address this challenge, future studies should focus on employing solubilizing agents and developing specific formulations to enhance the solubility and bioavailability of these agents. In addition, to fully validate the findings from our *in silico* and *in vitro* analyses, evaluating the expression of HIF1A and downstream targets at mRNA or protein level is recommended.

Conclusion

Our study reveals, for the first time, that MS-275 and novel analogs interacted with HIF-1α PAS-B domain and induced toxic effects on ATL cells in hypoxic condition. These findings hold promise for developing new drugs targeting hypoxia-induced changes in ATL. Further *in vitro* and preclinical studies are required to support the role of MS-275 and analogs as innovative agents for ATL.

Authors' contribution

S. Goudarzi, M. Vosough Ghanbari and J. Rohani carried out the experiments and analysis, R. Ghodsi advised the project and provided research materials, F.B. Rassouli designed and supervised the project and revised the manuscript.

Disclosure statement

No potential conflict of interest was reported by the author(s).

Funding

This study was financially supported by Mashhad University of Medical Sciences and Ferdowsi University of Mashhad.

ORCID

Fatemeh B. Rassouli http://orcid.org/0000-0003-1889-0964

Data availability statement

The data that support the findings of this study are available on request from the corresponding authors.

References

[1] Xia C, Tao Y, Li M, et al. Protein acetylation and deacetylation: an important regulatory modification in gene transcription. Exp Ther Med. 2020;20(4):2923–2940. doi: 10.3892/etm.2020.9073.

[2] Parveen R, Harihar D, Chatterji BP. Recent histone deacetylase inhibitors in cancer therapy. Cancer. 2023;129(21):3372–3380. doi: 10.1002/cncr.34974.

[3] Marks PA. Discovery and development of SAHA as an anticancer agent. Oncogene. 2007;26(9):1351–1356. doi: 10.1038/sj.onc.1210204.

[4] Qian X, Ara G, Mills E, et al. Activity of the histone deacetylase inhibitor belinostat (PXD101) in preclinical models of prostate cancer. Int J Cancer. 2008; 122(6):1400–1410. doi: 10.1002/ijc.23243.

[5] Fournel M, Bonfils C, Hou Y, et al. MGCD0103, a novel isotype-selective histone deacetylase inhibitor, has broad spectrum antitumor activity in vitro and in vivo. Mol Cancer Ther. 2008;7(4):759–768. doi: 10.1158/1535-7163.MCT-07-2026.

[6] Laubach JP, Moreau P, San-Miguel JF, et al. Panobinostat for the treatment of multiple myeloma. Clin Cancer Res. 2015;21(21):4767–4773. doi: 10.1158/1078-0432.CCR-15-0530.

[7] Zhang L, Zhang J, Jiang Q, et al. Zinc binding groups for histone deacetylase inhibitors. J Enzyme Inhib Med Chem. 2018;33(1):714–721. doi: 10.1080/14756366.2017.1417274.

[8] Omidkhah N, Eisvand F, Hadizadeh F, et al. Synthesis, cytotoxicity, pan-HDAC inhibitory activity and docking study of N-(2-Aminophenyl)-2-arylquinoline-4- and N-(2-Aminophenyl)-2-arylbenzo[h]-quinoline-4-carboxamides. Chem Select. 2022b;7(29): e202201239.

[9] Omidkhah N, Hadizadeh F, Abnous K, et al. Synthesis, structure activity relationship and biological evaluation of a novel series of quinoline–based benzamide derivatives as anticancer agents and histone deacetylase (HDAC) inhibitors. J Mol Struct. 2022a; 1267:133599. doi: 10.1016/j.molstruc.2022.133599.

[10] Fandy TE, Herman JG, Kerns P, et al. Early epigenetic changes and DNA damage do not predict clinical response in an overlapping schedule of 5-azacytidine and entinostat in patients with myeloid malignancies. Blood. 2009;114(13):2764–2773. doi: 10.1182/blood-2009-02-203547.

[11] Buglio D, Younes A. Histone deacetylase inhibitors in Hodgkin lymphoma. Invest New Drugs. 2010;28 Suppl 1(Suppl 1):S21–S7. doi: 10.1007/s10637-010-9588-y.

[12] Copeland A, Buglio D, Younes A. Histone deacetylase inhibitors in lymphoma. Curr Opin Oncol. 2010; 22(5):431–436. doi: 10.1097/CCO.0b013e32833d5954.

[13] Jóna A, Khaskhely N, Buglio D, et al. The histone deacetylase inhibitor entinostat (SNDX-275) induces apoptosis in Hodgkin lymphoma cells and synergizes with Bcl-2 family inhibitors. Exp Hematol. 2011;39(10): 1007–1017.e1. doi: 10.1016/j.exphem.2011.07.002.

[14] Zhou Z, Fang Q, Li P, et al. Entinostat combined with Fludarabine synergistically enhances the induction of apoptosis in TP53 mutated CLL cells via the HDAC1/HO-1 pathway. Life Sci. 2019;232:116583. doi: 10.1016/j.lfs.2019.116583.

[15] Wang B, Lyu H, Pei S, et al. Cladribine in combination with entinostat synergistically elicits anti-proliferative/anti-survival effects on multiple myeloma cells. Cell Cycle. 2018;17(8):985–996. doi: 10.1080/15384101.2018.1464849.

[16] Khanlari M, Ramos JC, Sanchez SP, et al. Adult T-cell leukemia/lymphoma can be indistinguishable from other more common T-cell lymphomas. The University of Miami experience with a large cohort of cases. Mod Pathol. 2018;31(7):1046–1063. doi: 10.1038/s41379-018-0037-3.

[17] Nosaka K, Crawford B, Yi J, et al. Systematic review of survival outcomes for relapsed or refractory adult T-cell leukemia-lymphoma. Eur J Haematol. 2022; 108(3):212–222. doi: 10.1111/ejh.13728.

[18] Tsukasaki K, Marçais A, Nasr R, et al. Diagnostic approaches and established treatments for adult T cell leukemia lymphoma. Front Microbiol. 2020;11: 1207. doi: 10.3389/fmicb.2020.01207.

[19] Zhao Y, Xing C, Deng Y, et al. HIF 1alpha signaling: essential roles in tumorigenesis and implications in targeted therapies. Genes Dis. 2023;11(1):234–251. doi: 10.1016/j.gendis.2023.02.039.

[20] McNamee EN, Korns Johnson D, Homann D, et al. Hypoxia and hypoxiainducible factors as regulators of T cell development, differentiation, and function. Immunol Res. 2013;55(1-3):58–70. doi: 10.1007/s12026-012-8349-8.

[21] Matolay O, Méhes G. Sustain, adapt, and overcome-hypoxia associated changes in the progression of lymphatic neoplasia. Front Oncol. 2019;9:1277. doi: 10.3389/fonc.2019.01277.

[22] Corzo CA, Condamine T, Lu L, et al. HIF-1alpha regulates function and differentiation of myeloid-derived suppressor cells in the tumor microenvironment. J Exp Med. 2010;207(11):2439–2453. doi: 10.1084/jem.20100587.

[23] Facciabene A, Peng X, Hagemann IS, et al. Tumour hypoxia promotes tolerance and angiogenesis via CCL28 and T(reg) cells. Nature. 2011;475(7355): 226–230. doi: 10.1038/nature10169.

[24] Kobayashi S, Nakano K, Watanabe E, et al. CADM1 expression and stepwise downregulation of CD7 are closely associated with clonal expansion of HTLV-I-infected cells in adult T-cell leukemia/lymphoma. Clin Cancer Res. 2014;20(11):2851–2861. doi: 10.1158/1078-0432.CCR-13-3169.

[25] Hamano R, Wu X, Wang Y, et al. Characterization of MT-2 cells as a human regulatory T cell-like cell line. Cell Mol Immunol. 2015;12(6):780–782. doi: 10.1038/cmi.2014.123.

[26] Zhang Q, Wang S, Chen J, et al. Histone deacetylases (HDACs) guided novel therapies for T-cell lymphomas. Int J Med Sci. 2019;16(3):424–442. doi: 10.7150/ijms.30154.

[27] Wang JC, Kafeel MI, Avezbakiyev B, et al. Histone deacetylase in chronic lymphocytic leukemia. Oncol. 2011;81(5-6):325–329. doi: 10.1159/000334577.

[28] Zimmerman B, Sargeant A, Landes K, et al. Efficacy of novel histone deacetylase inhibitor, AR42, in a mouse model of, human T-lymphotropic virus type 1 adult T cell lymphoma. Leuk Res. 2011;35(11): 1491–1497. doi: 10.1016/j.leukres.2011.07.015.

[29] Yu P, Petrus MN, Ju W, et al. Augmented efficacy with the combination of blockade of the Notch-1 pathway, bortezomib and romidepsin in a murine MT-1 adult T-cell leukemia model. Leukemia. 2015; 29(3):556–566. doi: 10.1038/leu.2014.241.

[30] Chen J, Zhang M, Ju W, et al. Effective treatment of a murine model of adult T-cell leukemia using depsipeptide and its combination with unmodified daclizumab directed toward CD25. Blood. 2009;113(6):1287–1293. doi: 10.1182/blood-2008-04-149658.

[31] Ramos JC, Lossos IS. Newly emerging therapies targeting viral-related lymphomas. Curr Oncol Rep. 2011;13(5):416–426. doi: 10.1007/s11912-011-0186-8.

[32] Stuver R, Horwitz SM, Epstein-Peterson ZD. Treatment of adult T-cell leukemia/lymphoma: established paradigms and emerging directions. Curr Treat Options Oncol. 2023;24(8):948–964. doi: 10.1007/s11864-023-01111-1.

[33] Key J, Scheuermann TH, Anderson PC, et al. Principles of ligand binding within a completely buried cavity in HIF2alpha PAS-B. J Am Chem Soc. 2009; 131(48):17647–17654. doi: 10.1021/ja9073062.

[34] Cardoso R, Love R, Nilsson CL, et al. Identification of Cys255 in HIF-1α as a novel site for development of covalent inhibitors of HIF-1α/ARNT PasB domain protein-protein interaction. Protein Sci. 2012;21(12): 1885–1896. doi: 10.1002/pro.2172.

[35] Zhou L, Ruvolo VR, McQueen T, et al. HDAC inhibition by SNDX-275 (Entinostat) restores expression of silenced leukemia-associated transcription factors Nur77 and Nor1 and of key pro-apoptotic proteins in AML. Leukemia. 2013;27(6):1358–1368. doi: 10.1038/leu.2012.366.

[36] Singh A, Chang T-Y, Kaur N, et al. CAP rigidification of MS-275 and chidamide leads to enhanced antiproliferative effects mediated through HDAC1, 2 and tubulin polymerization inhibition. Eur J Med Chem. 2021; 215:113169. doi: 10.1016/j.ejmech.2021.113169.